JPE 18-3-26

https://doi.org/10.6113/JPE.2018.18.3.923
ISSN(Print): 1598-2092 / ISSN(Online): 2093-4718

EMI Noise Reduction with New Active Zero State PWM for Integrated Dynamic Brake Systems

Jae-Hyuk Baik*, Sang-Won Yun**, Dong-Sik Kim***, Chun-Ki Kwon****, and Ji-Yoon Yoo†

†,*School of Electrical Engineering, Korea University, Seoul, Korea
**EBS Center, Global R&D, Mando Corporation, Gyeonggi-do, Korea
***Department of Electrical Engineering, Soonchunhyang University, Asan, Korea
****Department of Medical IT Engineering, Soonchunhyang University, Asan, Korea

Abstract

Based on the application of an integrated dynamic brake (IDB) system that uses a PWM inverter fed-AC motor drive to operate the piston, a new active zero state PWM (AZSPWM) is proposed to improve the stability and reliability of the IDB system by suppressing the conducted electro-magnetic interference (EMI) noise under a wide range of load torque. The new AZSPWM reduces common-mode voltage (CMV) by one-third when compared to that of the conventional space vector PWM (CSVPWM). Although this method slightly increases the output current ripple by reducing the CMV, like the CSVPWM, it can be used within the full range of the load torque. Further, unlike other reduced common-mode voltage (RCMV) PWMs, it does not increase the switching power loss. A theoretical analysis is presented and experiments are performed to demonstrate the effectiveness of this method.

Key words: Active zero state PWM (AZSPWM), Common-mode current (CMC), Common-mode voltage (CMV), Electro-magnetic interference (EMI), Integrated dynamic brake (IDB), Reduced common-mode voltage PWM (RCMV-PWM)

I. INTRODUCTION

With the evolution of internal combustion engines to electric vehicles (EVs), several changes are required, one of which is the braking system. The conventional vacuum brake amplifies pedal pressure using vacuum generated by the engine. However, since EVs have no such engine, conventional vacuum brake is no longer applicable [1]-[3]. For this reason, an integrated dynamic brake (IDB) system has been developed [4].

However, in an IDB system, a PWM inverter fed-AC motor drive is used for the operation of the piston. However, this suffers from the common-mode voltage (CMV) problem. A CMV with sharp edges produces a high CMC. This may lead to motor bearing failures and electro-magnetic interference (EMI) noise that causes a nuisance trip of the inverter drive or interference with other electronic equipment [5], [6].

Consequently, EMI may seriously degrade the stability and reliability of an IDB system, which is directly related to driver safety [7]. Therefore, it is necessary to study approaches to reduce EMI noise from IDB systems. In addition, it is imperative to ensure the stability, reliability and robustness of IDB systems against EMI.

To cope with the CMV problem in PWM inverter fed-AC motor drives, many researchers have proposed various methods. Hardware approaches include common-mode chokes [8], [9], 4-phase inverters [10], passive/active cancellation circuits [11]-[15], and passive/active filters [16]-[18]. Software approaches include switching pattern modification of the conventional space vector PWM (CSVPWM) for a reduction of the CMV in addition to other approaches [19]-[22]. Using these approaches known as reduced common-mode voltage (RCMV) PWM, the CMV is reduced from $\pm V_{dc}/2$ of the CSVPWM to $\pm V_{dc}/6$. Unlike hardware approaches, software approaches do not need an additional components in the

Manuscript received Sep. 14, 2017; accepted Nov. 18, 2017
Recommended for publication by Associate Editor Yijie Wang.
†Corresponding Author: jyyoo@korea.ac.kr
Tel: +82-2-3290-3227, Korea University
*School of Electrical Engineering, Korea University, Korea
**EBS Center, Mando Corporation, Korea
***Dept. of Electrical Engineering, Soonchunhyang University, Korea
****Dept. of Medical IT Engineering, Soonchunhyang University, Korea

system. Thus, they are more attractive in terms of mounting space, fuel efficiency and economy [20]-[22]. Because of these advantages, the application of RCMV-PWMs to three-phase four-leg inverters and dual-inverters has also been studied [23], [24]. It is assumed that the new AZSPWM in [22] is a potential candidate to reduce both the CMV and switching power loss among the RCMV-PWMs with a full modulation index.

The final objective of this study is the reduction of both the switching power loss and EMI by applying the new AZSPWM to the IDB system. In this study, the CMV, total switching number and voltage linearity are analyzed, while the output phase current, CMV and EMI performances are evaluated under a wide range of load torque. From the experimental results and analysis, it is confirmed that the EMI noise reduction using the new AZSPWM is valid in all of the load torque regions of the IDB system.

II. IDB System

The structure of the IDB system is shown in Fig. 1. When a driver applies the brake pedal, data from the pedal travel sensor (PTS) is transferred to the ECU, which calculates the motor torque and speed. Then, the rotational motion of the motor is transformed to rectilinear motion by a worm gear, and it applies or releases pressure on the piston.

When the electrical relationship of the IDB is considered, parasitic elements exist within the system, such as stray or parasitic capacitances between two conductors (e.g., between the power module of the IGBT/MOSFET and the heat sink or ground plane; between the power cable and the ground plane; and between the motor frame and the stator windings) and parasitic inductance (e.g., electric wires). The stray capacitance leads to common-mode (CM) conducted noise being unintentionally generated in the system, which can be expressed by (1). Parasitic inductance generates differential mode (DM) conducted noise, as expressed by (2). Thus, if the value of the parasitic elements is high and/or the switching is fast (high dv/dt and high di/dt), the EMI will be increased.

$$i_c = C_p \frac{dv}{dt} \tag{1}$$

$$v_d = L_p \frac{di}{dt} \tag{2}$$

The main source of EMI noise in the PWM inverter fed-AC motor drive of a IDB system is shown in Fig. 2. The high dv/dt of the CMV due to the rapid switching operations (20 kHz in this system) produces a considerable amount of CMC, which flow through the parasitic capacitance between the motor frame and stator windings. These currents enter the chassis ground of the vehicle, which is connected to the motor frame. This may lead to motor bearing failures, EMI noise that causes a nuisance trip of the inverter drive or interference with other electronic equipment. Therefore, it is imperative to reduce EMI noise from the PWM inverter fed-AC motor drive of an IDB system to ensure stability and reliability.

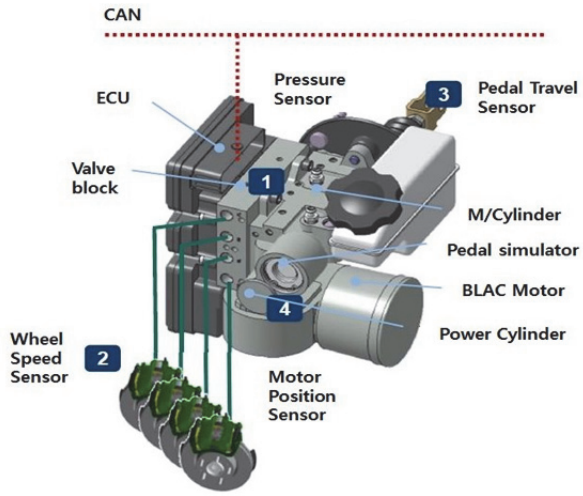

Fig. 1. Structure of the IDB system.

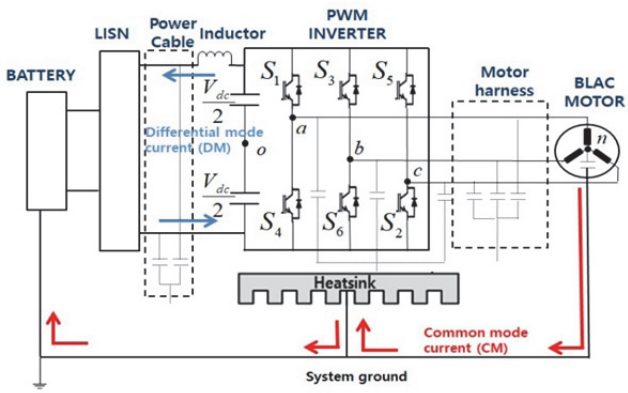

Fig. 2. PWM inverter fed-AC motor drive of an IDB system.

III. New AZSPWM Method

A. Common-Mode Voltage

CMV is defined as the potential difference between the star point of a load and the center of the dc-link of a three-phase inverter. From the three-phase balance condition, CMV can be calculated as:

$$V_{no} = V_{cm} = \frac{V_{ao} + V_{bo} + V_{co}}{3} \tag{3}$$

A three-phase inverter has eight switching states and may be expressed as voltage vectors in the d-q plane. Among these voltage vectors, V_0 and V_7 are known as zero voltage vectors while the vectors from V_1 to V_6 are known as active voltage vectors.

Table I shows the CMV according to the voltage vectors of a three-phase inverter. The formations of the voltage vectors and CMV for the CSVPWM and the new AZSPWM, when synthesizing the reference voltage vector located in sector

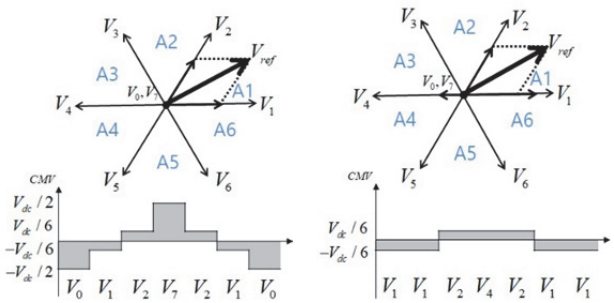

Fig. 3. Formation of voltage vectors in the d-q plane and CMV with: (a) CSVPWM; (b) new AZSPWM.

A1, are shown in Fig. 3. The switching sequences of the CSVPWM and the new AZSPWM for each of the sectors are listed in Table II. While the CSVPWM utilizes a combination of active voltage vectors and zero voltage vectors to synthesize the reference voltage vector, the new AZSPWM uses only active voltage vectors. From these results, the range of the CMV is significantly reduced from $-V_{dc}/2 \le V_{cm} \le V_{dc}/2$ of the CSVPWM to $-V_{dc}/6 \le V_{cm} \le V_{dc}/6$ as with other RCMV-PWMs.

B. Number of Switchings

For both the CSVPWM and the RCMV-PWMs, the utilized voltage vectors can synthesize the same reference voltage vector on average. However, the use of the voltage vector causes switching related to the heat performance and energy efficiency of the system. Therefore, the number of switchings should be considered. The total number of switchings is divided into the number of switchings at switching sequence step changes, and the number of switching at sector changes. All of the RCMV-PWMs except for the NSPWM [20] and the new AZSPWM have a higher total number of switchings than that of the CSVPWM. Because the new AZSPWM has the same number of switchings at sequence step changes and sector changes when compared to the CSVPWM, it does not decrease the heat performance or fuel efficiency of the system unlike other RCMV-PWMs [21], [22].

C. Voltage Linearity

Each PWM has a specific voltage linearity range. The voltage linearity range is an important characteristic of PWM since it is related to the low-frequency harmonics of the output voltage, which results in significant distortion of the motor current and torque. Therefore, it is desirable to have a wide voltage linearity range. AZSPWMs, including the new AZSPWM, have the same voltage linearity characteristics as the CSVPWM. However, other RCMV-PWMs have limitations of the dc-voltage utilization (not feasible for a specific region) [20], [21].

From the view point of both the CMV and the switching power loss, the NSPWM is attractive for motor control. Nevertheless, because the NSPWM has a limitation on the voltage linearity range, it is not suitable for IDB systems that require variable torque control. Among the remaining RCMV-PWMs, the new AZSPWM reduces the CMV to $V_{dc}/6$ as is the case with other RCMV-PWMs. In addition, it has the lowest number of switchings. Furthermore, it has the full voltage linearity range. Thus, the new AZSPWM is the most appropriate choice to control the AC motors of IDB systems and to reduce both the CMV and switching power loss of the system. Therefore, it is expected that the new AZSPWM will improve the stability and reliability of IDB systems through an improvement of the fuel efficiency, heat performance and EMI performance.

TABLE I
INVERTER POLE VOLTAGE AND CMV BY SWITCHING STATE

Switching state		V_{an}	V_{bn}	V_{cn}	CMV
Zero voltage vector	$V_0(0,0,0)$	−Vdc/2	−Vdc/2	−Vdc/2	−Vdc/2
	$V_7(1,1,1)$	+Vdc/2	+Vdc/2	+Vdc/2	+Vdc/2
Active voltage vector	$V_1(1,0,0)$	+Vdc/2	−Vdc/2	−Vdc/2	−Vdc/6
	$V_2(1,1,0)$	+Vdc/2	+Vdc/2	−Vdc/2	+Vdc/6
	$V_3(0,1,0)$	−Vdc/2	+Vdc/2	−Vdc/2	−Vdc/6
	$V_4(0,1,1)$	−Vdc/2	+Vdc/2	+Vdc/2	+Vdc/6
	$V_5(0,0,1)$	−Vdc/2	−Vdc/2	+Vdc/2	−Vdc/6
	$V_6(1,0,1)$	+Vdc/2	−Vdc/2	+Vdc/2	+Vdc/6

TABLE II
SWITCHING PATTERNS FOR THE CSVPWM AND THE NEW AZSPWM

SECTOR	A1	A2	A3	A4	A5	A6
CSVPWM	0127210	0327230	0347430	0547450	0567650	0167610
NEW AZSPWM	12421	1234321	13431	15451	1654561	16561

IV. CURRENT RIPPLE

In each type of PWM, the utilized voltage vectors can synthesize the same reference voltage vector on average. However, there is an error voltage vector between the instantaneous applied voltage vector and the reference voltage vector. This error is said to be responsible for the ripple content in the load current [25], [26], which is different for each type of PWM [19], [21]. For a given reference voltage vector located in sector A1, the error voltage vectors and the trajectories of both the CSVPWM and the new AZSPWM are shown in Fig. 4. The current ripple is the same as the trajectory of the error volt-second vector [25], [26]. The d-q axes current ripple in the time domain are shown in Fig. 5. The value of the q-axis ripple at the switching instants is given in terms of Q_1, Q_2, Q_{z0}, Q_{z1} and Q_{z4} while that of the d-axis ripple is given in terms of D_1, D_{z1} and D_{z4}. The quantities Q and D are as defined in (4) and (5), respectively.

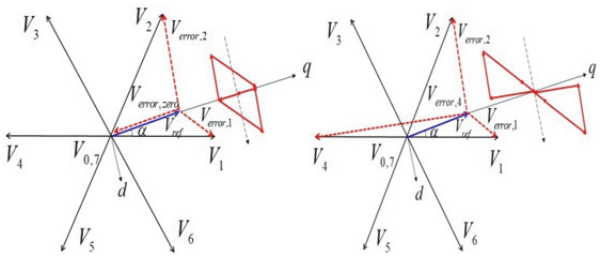

(a) (b)

Fig. 4. Error voltage vectors and their trajectory in the d-q axes: (a) CSVPWM; (b) New AZSPWM.

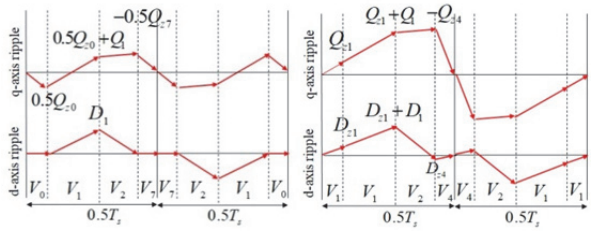

(a) (b)

Fig. 5. d-q axes current ripple in the time domain: (a) CSVPWM; (b) New AZSPWM.

$$
\begin{aligned}
Q_1 &= (\cos\alpha - V_{ref})T_1 \\
Q_2 &= (\cos(60-\alpha) - V_{ref})T_2 \\
Q_{z0} &= Q_{z7} = -V_{ref}T_0/2 \\
Q_{z1} &= (\cos\alpha - V_{ref})T_0/2 \\
Q_{z4} &= (-\cos\alpha - V_{ref})T_0/2
\end{aligned} \tag{4}
$$

$$
\begin{aligned}
D_1 &= \sin\alpha T_1 \\
D_{z1} &= \sin\alpha T_0/2 \\
D_{z4} &= -\sin\alpha T_0/2
\end{aligned} \tag{5}
$$

From the equations, it is observed that the direction of the error voltages determine the slope of the current trajectory. It can also be seen that the dwell times of the voltage vectors determine the magnitude of the current ripple.

In the new AZSPWM, opposite active voltage vectors (V1 and V4) are applied for the same duration instead of zero voltage vectors (V0 and V7) when synthesizing the reference voltage vector. The error voltage vectors of V1 and V4 increase the peak value of the d-q axes current ripple as shown in Fig. 5. Consequently, these ripple contents appear in the output phase current. From this analysis, it is expected that the ripple of the output phase current of the new AZSPWM is slightly greater than that of the CSVPWM. This can be seen from the following experimental results, where the harmonic contents are also discussed.

V. Experimental Results

To verify the validity of the new AZSPWM and to compare it with the CSVPWM, experimental tests were performed. A hardware setup of the experiment is shown in Fig. 6. The setup consists of a 12 V DC battery, a line impedance stabilization network (LISN), an IDB system (VSI, MCU (TRICORE277, INFINEON), G/D and a BLAC motor), a load motor, and a laptop. The BLAC motor used in this experiment has the following rated values: 1 kW, 2.74 N·m, 8-pole and 1500 RPM along with the following parameters: R_s = 14.4 mΩ, L_d = 35 μH, L_q = 48 μH and J = 39.8 kgm^2. During the test, the switching frequency was 20 kHz. The test was performed at T_L = 0.15 N·m, T_L = 1 N·m and T_L = 2 N·m with 50 RPM to analyze the effects of the new AZSPWM on the output current and EMI level under a wide load torque range. The vector control scheme used in this test is shown in Fig. 7. Experimental waveforms were obtained using an oscilloscope (WAVERUNNER HRO 64Zi, LECROY) and an EMI receiver (ESPI7, ROHDE&SCHWARZ).

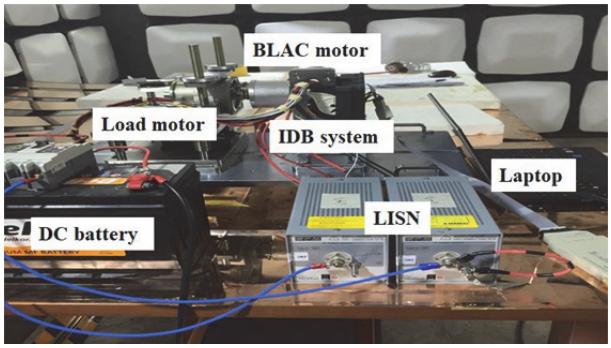

Fig. 6. Hardware setup.

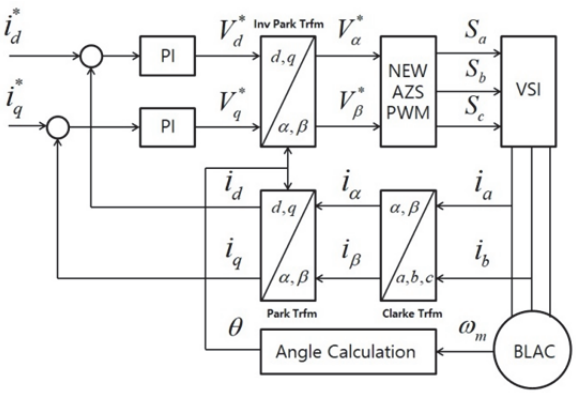

Fig. 7. Block diagram of the vector control scheme.

Figs. 8 and 9 show experimental waveforms of the output current of phase-a according to the amplitude of the load torque, when applying the CSVPWM and the new AZSPWM, respectively. It is shown that for the new AZSPWM, the output current ripple is slightly higher than that of the CSVPWM under all load torque conditions. This is because the d-q axes current ripples by the instantaneous voltage error of the new AZSPWM are greater than those of the CSVPWM, as described in the previous section. Furthermore, it is observed that the peak value of the phase current increases in proportion to the amplitude of the load torque. In addition,

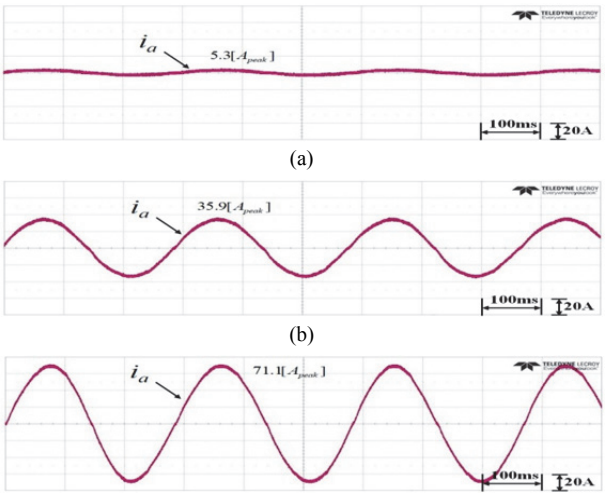

Fig. 8. Experimental waveforms of the output phase current in the CSVPWM: (a) T_L=0.15N·m; (b) T_L=1N·m; (c) T_L=2N·m.

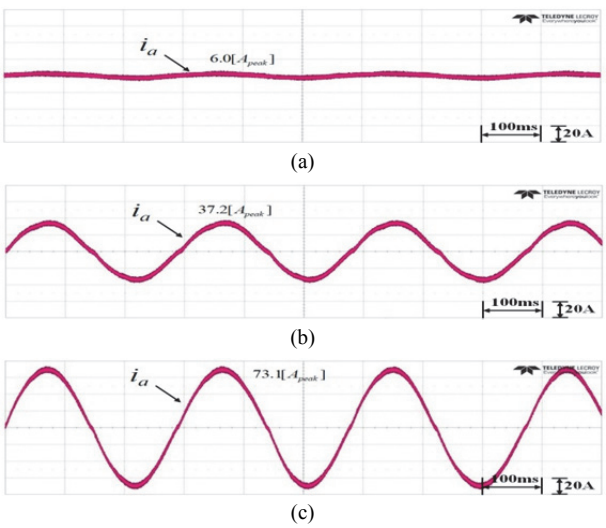

Fig. 9. Experimental waveforms of the output phase current in the new AZSPWM: (a) T_L=0.15N·m; (b) T_L=1N·m; (c) T_L= 2N·m.

the peak value of the AZSPWM is slightly higher than that of the CSVPWM under all load torque conditions. This can also be an effect of the ripple contents.

The FFT of the output current is discussed as a reference. The amplitude at the fundamental frequency (3.3 Hz) of the CSVPWM is slightly greater than that of the new AZSPWM. On the other hand, the amplitude at the switching frequency (20 kHz) of the new AZSPWM is greater than that of the CSVPWM. This is because the effects of the d-q axes current ripple contents (described in the previous section) mainly appeared at the switching frequency and there is no significant difference in the amplitude at double the switching frequency (40kHz). Both in the CSVPWM and the AZSPWM, the amplitude at the fundamental frequency increases in proportion to the amplitude of the load torque. However, increases in the amplitude at the switching frequency and the

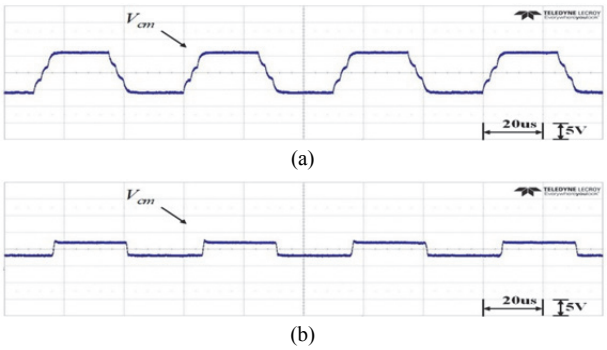

Fig. 10. Experimental waveforms of the CMV at T_L=0.15N·m: (a) CSVPWM; (b) New AZSPWM.

double switching frequency are relatively very small. Therefore, whenthe amplitude of the load torque increases, the ratio of the harmonic contents to the fundamental contents decreases. As a result, the effects of harmonics on a system can be considered negligible.

Fig. 10 shows experimental waveforms of the CMV when applying the CSVPWM and the new AZSPWM. When the new AZSPWM is utilized, the peak value of the CMV is reduced from 6 V to 2 V, corresponding to 1/3 of that of the CSVPWM. Further, the number of steps of CMV is reduced. The new AZSPWM has a different number of steps of CMV depending on the sector. However, in this case, the number of steps is reduced from 6 to 2 when the reference voltage is synthesized once. It reduces the RMS value of the CMV and the number of pulses of the CMC, which reduces the RMS value of the CMC. Moreover, when the applied time of one of the two active vectors that form the switching patterns is considerably small in the CSVPWM algorithm, the dv/dt of the CMV can be rapidly increased, leading to an increase in the peak value of the CMC. However, in the new AZSPWM, since the CMV alternately rises and falls, there is no risk that the peak value of the CMC will increase. In the fixed DC voltage system, the peak value of the CMV is only dependent on the switching states (voltage vector) as defined in (3). Therefore, the new AZSPWM can always reduce the peak value of the CMV to 1/3 in all of the load torque regions. As a result, the new AZSPWM reduces the peak and RMS values of both the CMV and the CMC, leading to a reduction in the conducted EMI noise.

The EMI test was also conducted to analyze the effect of the new AZSPWM on the EMI performance of an IDB system under a wide load torque range. A conducted emission test along power lines with respect to standard $CISPR_{25}$ was applied to electronic/electrical components intended for use in vehicles. The conducted voltage (+) was measured by the voltage method. Figs. 11 and 12 show EMI test results according to the amplitude of the load torque when applying the CSVPWM and the new AZSPWM, respectively. In these figures, the blue lines represent the measured peak value and the red lines represent the peak limits set by $CISPR_{25}$ class 4.

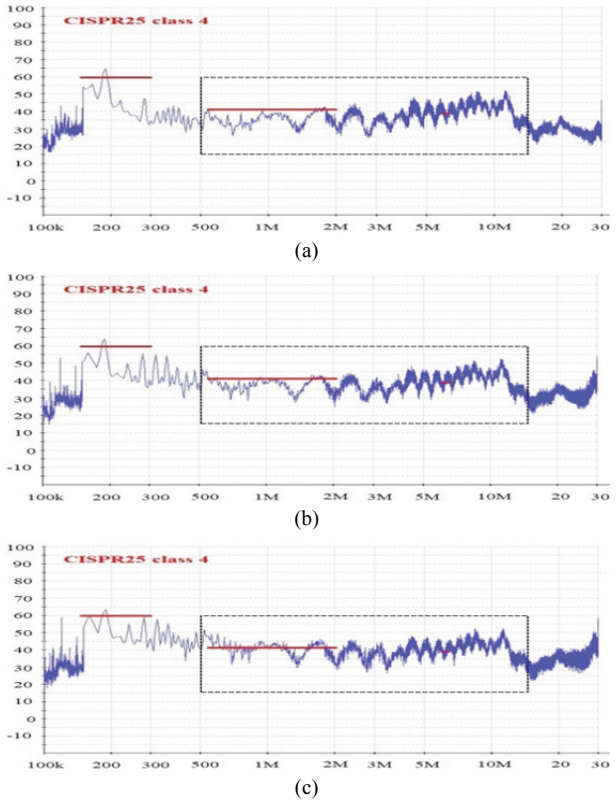

Fig. 11. Measured waveform of the conducted EMI level in the CSVPWM: (a) T_L=0.15N·m; (b) T_L=1N·m; (c) T_L=2N·m.

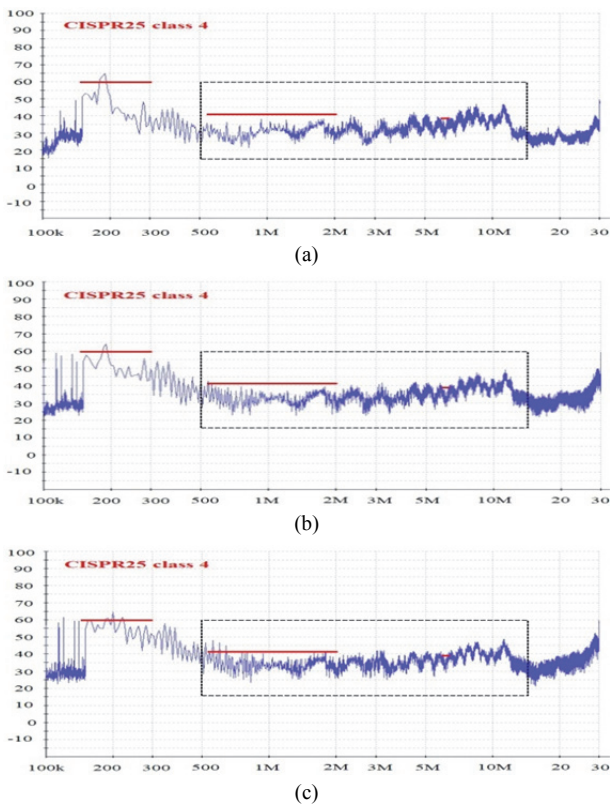

Fig. 12. Measured waveform of conducted EMI level in NEW AZSPWM: (a) T_L=0.15N·m; (b) T_L=1N·m; (c) T_L=2N·m.

In the case of T_L = 0.15 N·m [Figs. 11(a) and 12(a)], it was observed that when the new AZSPWM was applied, in the 500 kHz–15 MHz frequency range, the EMI level was reduced at least by 1 dBμV and by a maximum of 6 dBμV. However, when the CSVPWM was applied, only a small amount of fluctuation was observed in the other frequency ranges. Given that the new AZSPWM is a method to reduce CM noise by decreasing the peak value and the RMS value of the CMV and CMC, it can be considered that the effect of CM noise is predominate in the 500 kHz–15 MHz frequency range in the IDB system under the experimental conditions.

When the amplitude of the load torque is increased from T_L = 0.15 N·m to T_L = 1 N·m [Figs. 11(a) and 11(b), Figs. 12(a) and 12(b)], the EMI level increased by a minimum of 1 dBuV and a maximum of 8 dBuV in almost all frequency ranges [100 kHz–30 MHz] in both the CSVPWM and the new AZSPWM, respectively. The variation was particularly pronounced in the 100 kHz–1 MHz and 10 MHz–30 MHz frequency ranges. This can be attributed to an increase in the DM and CM noise due to an increase in the output phase current. On the other hand, when the new AZSPWM was applied, the EMI level was reduced when compared with the CSVPWM, which is similar to the case of T_L = 0.15 N·m [Figs. 11(b) and 12(b)]. Since the CM noise level reduction technique of the new AZSPWM mainly depends on $C_p \times dV_{cm}/dt$, it is possible to reduce similar amounts of EMI levels where CM noise predominates even though the amplitude of the load torque increases.

When the amplitude of the load torque is increased from T_L = 1 N·m to T_L = 2 N·m [Figs. 11(b) and 11(c), Figs. 12(b) and 12(c)], as in the previous case, the EMI level increased by a minimum of 1 dBμV and a maximum of 6 dBμV in almost all frequency ranges in both the CSVPWM and AZSPWM, respectively. Correspondingly, when the AZSPWM was applied, the EMI level where the CM noise predominates in this system is reduced to a maximum of 6 dBμV when compared to when the CSVPWM was applied [Figs. 11(c) and 12(c)].

In a IDB system under these experimental conditions, when the amplitude of the load torque increases, the EMI level tends to increase in almost all of the frequency ranges in both the CSVPWM and the new AZSPWM. However, an amount of the EMI level can always be reduced when the effect of CM noise predominates (500 kHz–15 MHz in this system) and the new AZSPWM is applied. At the same time, in all of the load torque regions, the measured values of the new AZSPWM were almost lower than the limits set by $CISPR_{25}$ class 4. As a result, it is confirmed that the new AZSPWM is valid in all load torque regions.

VI. Conclusion

In this paper, the application of a new AZSPWM to an IDB system was described. The new AZSPWM improves the

stability and the reliability of the IDB system by suppressing the conducted EMI noise. From the analysis, it was confirmed that the new AZSPWM reduced CMV by one-third when compared with the CSVPWM. In addition, it had the lowest total switching number among the RCMV-PWMs with a full modulation index. Although the new AZSPWM increased the output current ripple (especially the harmonics at the switching frequency) by reducing the CMV, the effect of the harmonics on the system was negligible since the amplitude of the load torque increased. Through experimental results, it was verified that the new AZSPWM improved the performance of the conducted EMI within the full range of load torque when compared to the CSVPWM. This method is a valid solution for designing the EMI characteristics of an IDB system.

REFERENCES

[1] J. W. Kim, S. Y. Ko, G. U. Lee, H. Yeo, P. G. Kim, and H. S. Kim, "Development of co-operative control algorithm for parallel HEV with electric booster brake during regenerative braking," *Proc. IEEE VPPC*, pp. 1-5, 2011.

[2] H. Yeo, C. Koo, W. Jung, D. Kim, and J. S. Cheon, "Development of smart booster brake systems for regenerative brake cooperative control," *SAE Technical Paper 2011-01-2356*, 2011.

[3] Z. Wang, L. Yu, Y. Wang, K. Wu, N. Pan, Jian Song, and L. Ma, "Design concepts of the four-wheel-independent electrohydraulic braking system," *SAE Technical Paper 2014-01-2537*, 2014.

[4] S. S. Han, "Integrated dynamic brake apparatus," U.S. Patent 0107629 A1, Apr. 21, 2016.

[5] B. Revol, J. Roude, J.-L. Schanen, and P. Loizelet, "EMI study of three-phase inverter-fed motor drives," *IEEE Trans. Ind. Appl.*, Vol. 47, No. 1, pp. 223-231, Jan./Feb. 2011.

[6] C. Jettanasen, "Analysis of conducted electromagnetic interference generated by PWM inverter Fed-AC motor drive," *Proc. IEEE ICEMS*, pp. 1-6, 2012.

[7] R. Limpert, *Brake Design and Safety*, SAE International, Chap. 10, 2011.

[8] A. Muetze, "Scaling issues for common-mode chokes to mitigate ground currents in inverter-based drive systems," *IEEE Trans. Ind. Appl.*, Vol. 45, No. 1, pp. 286-294, Jan./ Feb. 2009.

[9] D. Jiang, F. Wang, and J. Xue, "PWM impact on CM noise and AC CM choke for variable-speed motor drives," *IEEE Trans. Ind. Appl.*, Vol. 49, No. 2, pp. 963-972, Mar./Apr. 2013.

[10] A. L. Julian, G. Oriti, and T. A. Lipo, "Elimination of common-mode voltage in three-phase sinusoidal power converters," *IEEE Trans. Power Electron*., Vol. 14, No. 5, pp. 982-989, Sep. 1999.

[11] L. Xing and J. Sun, "Conducted common-mode EMI reduction by impedance balancing," *IEEE Trans. Power Electron*., Vol. 27, No. 3, pp. 1084-1089, Mar. 2012.

[12] C. Zhu and T. H. Hubing, "An active cancellation circuit for reducing electrical noise from three-phase AC motor drivers," *IEEE Trans. Electromagn. Compat.*, Vol. 56, No. 1, pp. 60-66, Feb. 2014.

[13] C. T. Morris, D. Han, and B. Sarlioglu, "Reduction of common mode voltage and conducted EMI through three-phase inverter topology," *IEEE Trans. Power Electron*., Vol. 32, No. 3, pp. 1720-1724, Mar. 2017.

[14] Di Han, Casey T. Morris, and B. Sarlioglu, "Common-mode voltage cancellation in PWM motor drives with balanced inverter topology," *IEEE Trans. Ind. Electron.*, Vol. 64, No. 4, pp. 2683-2688, Apr. 2017.

[15] S. Ogasawara, H. Ayano, and H. Akagi, "An active circuit for cancellation of common-mode voltage generated by a PWM inverter," *IEEE Trans. Power Electron*., Vol. 13, No. 5, pp. 835-841, Sep. 1998.

[16] H. Akagi and S. Tamura, "A passive EMI filter for eliminating both bearing current and ground leakage current from an inverter-driven motor," *IEEE Trans. Power Electron*., Vol. 21, No. 5, pp. 1094-1101, Sep. 2006.

[17] W. Wu, Y. Sun, Z. Lin, Y. He, M. Huang, F. Blaabjerg, and H. S. Chung, "A modified LLCL filter with the reduced conducted EMI noise," *IEEE Trans. Power Electron*., Vol. 29, No. 7, pp. 3393-3402, Jul. 2014.

[18] R. Guzman, L. G. de Vicuna, J. Morales, M. Castilla, and J. Miret, "Model-based active damping control for three-phase voltage source inverters with LCL filter," *IEEE Trans. Power Electron*., Vol. 32, No. 7, pp. 5637-5650, Jul. 2017.

[19] S. M. Ali, V. V. Reddy, and M. S. Kalavathi, "Simplified active zero state PWM algorithm for vector controlled induction motor drives for reduced common mode voltage," *Proc. IEEE ICRAIE*, pp. 1-7, 2014.

[20] E. Un and A. M. Hava, "A near-state PWM method with reduced switching losses and reduced common-mode voltage for three-phase voltage source inverters," *IEEE Trans. Ind. Appl.*, Vol. 45, No. 2, pp. 782-793, Mar./Apr. 2009.

[21] A. M. Hava and E. Un, "Performance analysis of reduced common-mode voltage PWM methods and comparison with standard PWM methods for three-phase voltage source inverters," *IEEE Trans. Power Electron.*, Vol. 24, No. 1, pp. 241-252, Jan. 2009.

[22] S. W. Yun, J. H. Baik, D. S. Kim, and J. Y. Yoo, "A new active zero state PWM algorithm for reducing the number of switchings," *J. Power Electron.*, Vol. 17, No. 1, pp. 88-95, Jan. 2017.

[23] M. Zhang, D. J. Atkinson, B. Ji, M. Armstrong, and M. Ma, "A near-state three-dimensional space vector modulation for a three-phase four-leg voltage source inverter," *IEEE Trans. Power Electron.*, Vol. 29, No. 11, pp. 5715-5726, Nov. 2014.

[24] J. Kalaiselvi and S. Srinivas, "Bearing currents and shaft voltage reduction in dual-inverter-fed open-end winding induction motor with reduced CMV PWM methods," *IEEE Trans. Ind. Electron.*, Vol. 62, No. 1, pp. 144-152, Jan. 2015.

[25] D. Casadei, G. Serra, A. Tani, and L. Zarri, "Theoretical and experimental analysis for the RMS current ripple minimization in induction motor drives controlled by SVM technique," *IEEE Trans. Ind. Electron.*, Vol. 51, No. 5, pp. 1056-1065, Oct. 2004.

[26] G. Narayanan, D. Zhao, H. K. Krishnamurthy, R. Ayyanar, and V. T. Ranganathan, "Space vector based hybrid PWM techniques for reduced current ripple," *IEEE Trans. Ind. Electron.*, Vol. 55, No. 4, pp. 1614-1627, Apr. 2008.

Jae-Hyuk Baik was born in Seoul, Korea, in 1989. He received his B.S. degree in Electrical and Information Engineering from the Seoul National University of Science and Technology, Seoul, Korea, in 2014. He is presently working towards his Ph.D. degree in Electrical Engineering from Korea University, Seoul, Korea. His current research interests include voltage-source inverters, pulse width modulation methods, and common-mode noise and its reduction methods in ac motors.

Sang-Won Yun was born in Seoul, Korea, in 1978. He received his B.S. degree in Electrical Engineering from Korea University, Seoul, Korea, in 2004, where he is presently working towards his Ph.D. degree. In 2004, he joined MANDO Corporation, where is presently developing an integrated dynamic brake ECU. His current research interests include the effects of motor control on EMC (Electro-Magnetic Compatibility).

Dong-Sik Kim was born in Seoul, Korea, on September 10, 1963. He received his B.S., M.S. and Ph.D. degrees in Electrical Engineering from Korea University, Seoul, Korea, in 1986, 1988 and 1992, respectively. In September 1992, he joined the Department of Electrical Engineering, Soonchunhyang University, Asan, Korea, where he is presently working as a Professor. His current research interests include web-based virtual laboratories, distance education, nonlinear robust control and intelligent control.

Chun-Ki Kwon received his M.S. degree from the Department of Electrical Engineering, Korea University, Seoul, Korea, in 1994; and his Ph.D. degree from the School of Electrical and Computer Engineering, Purdue University, West Lafayette, Indiana, in 2005. From July 2006 to February 2008, he was a Chief Engineer in the design of electric motor hybrid electric vehicles at Hyundai-Kia Motor Company. Since 2008, he has been a faculty member in the Department of Medical IT Engineering at Soonchunhyang University, Asan, Korea. His current research interests include the control and modeling of electric machines, medical engineering and rehabilitation devices.

Ji-Yoon Yoo received his B.S. and M.S. degrees in Electrical Engineering from Korea University, Seoul, Korea, in 1977 and 1983, respectively. He received his Ph.D. in Electrical Engineering from Waseda University, Tokyo, Japan, in 1987. From 1987 to 1991, he was an Assistant Professor in the Department of Electrical Engineering, Changwon National University, Changwon, Korea. He joined the Department of Electrical Engineering, Korea University, in 1991, where he has conducted research on the control of electric machines and drives as well as power electronics converters under major industrial and government contracts. His current research interests include the modeling, analysis and control of hybrid electric vehicle systems, BLDC motors and PM synchronous motors.